High output current in vertical polymer space-charge-limited transistor induced by self-assembled monolayer

Hsiao-Wen Zan, Yuan-Hsuan Hsu, Hsin-Fei Meng, Chian-Hao Huang, Yu-Tai Tao, and Wu-Wei Tsai

Articles you may be interested in

Sensitive gas sensor embedded in a vertical polymer space-charge-limited transistor
Appl. Phys. Lett. **101**, 023303 (2012); 10.1063/1.4734498

Multiple-trapping in pentacene field-effect transistors with a nanoparticles self-assembled monolayer
AIP Advances **2**, 022128 (2012); 10.1063/1.4720399

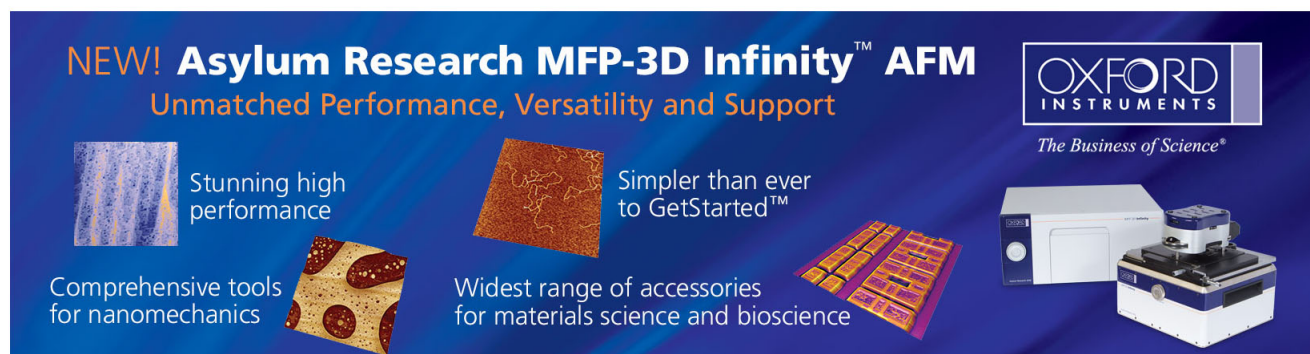High-performance space-charge-limited transistors with well-ordered nanoporous aluminum base electrode
Appl. Phys. Lett. **99**, 093306 (2011); 10.1063/1.3632045

Photopatternable self-assembled monolayers as micron scale templates for polymer based field effect transistors
Appl. Phys. Lett. **94**, 013502 (2009); 10.1063/1.3064158

Polymer space-charge-limited transistor
Appl. Phys. Lett. **88**, 223510 (2006); 10.1063/1.2207838

High output current in vertical polymer space-charge-limited transistor induced by self-assembled monolayer

Hsiao-Wen Zan,[1,a)] Yuan-Hsuan Hsu,[2] Hsin-Fei Meng,[2,a)] Chian-Hao Huang,[1] Yu-Tai Tao,[3] and Wu-Wei Tsai[1]

[1]*Department of Photonics and Institute of Electro-Optical Engineering, National Chiao Tung-University, 1001, Ta-Hsueh Rd, Hsinchu 300, Taiwan*
[2]*Institute of Physics, National Chiao Tung University, 1001, Ta-Hsueh Rd, Hsinchu 300, Taiwan*
[3]*Institute of Chemistry, Academia Sinica, Taipei 115, Taiwan*

We present a promising solution-processed vertical transistor which exhibits high output current, high on/off current ratio, and low operation voltage. Numerous poly(3-hexylthiophene) vertical channels are embedded in vertical nanometer pores. Treating the sidewalls of pores by self-assemble monolayer with long alkyl chains enhances the pore-filling and inter-chain order of poly (3-hexylthiophene). The channel current is therefore greatly increased. A grid metal inside the porous template controls the channel potential profile to turn on and turn off the vertical transistor. Finally, the transistor delivers an output current density as 50–110 mA/cm^2 at 2 V with an on/off current ratio larger than 10 000. © 2012 American Institute of Physics. [http://dx.doi.org/10.1063/1.4748284]

Solution-processed organic transistor is an emerging technology due to the low-cost and large-area fabrication. One important potential application is the driving transistor for the active-matrix organic light-emitting diode (OLED) display. Unlike liquid-crystal display, OLED requires a high current in order to achieve enough luminance. It is difficult for conventional organic field-effect transistor (FET) to deliver such high current with low operation voltage due to the poor mobility and long channel length. Vertical space-charge-limited transistor (SCLT) shows superior performance than FET due to the short vertical channel length.[1,2] So far the operation voltage is below 3 V, but the output current density is only around 5 mA/cm^2. In a simple vertical stacking with OLED of typical efficiency of 10 cd/A, such current density corresponds to luminance of only 500 cd/m^2, which is barely enough. For practical application, the vertical transistor should deliver a maximal current density of 50 mA/cm^2, from which a corresponding luminance of 5000 cd/m^2 is high enough by a large margin.

No matter in the horizontal channel of conventional FET or the vertical channel of SCLT, the transistor output current is controlled by the carrier mobility. In FET fabrication, self-assembled monolayer (SAM) treatment of the gate dielectric is commonly used to improve the mobility by tuning the organic semiconductor morphology. In-plane field-effect hole mobility in regioregular poly(3-hexylthiophene) (RR P3HT), one of the most promising conjugated polymers with the molecular structure shown in Fig. 1(a) is higher than 0.1 cm^2/Vs along the polymer backbone and the in-plane π-π orbital stacking and is lower than 2×10^{-4} cm^2/Vs when the π-π stacking direction is perpendicular to the current flow direction.[3,4] There are three possible orientations for the packing of P3HT chains. Edge-on orientation has in-plane π-π stacking direction and in-plane backbone direction. Face-on orientation represents that the π-π stacking

direction is perpendicular to the substrate. Vertical orientation exhibits vertically aligned backbone and possible in-plane π-π stacking.[5] For organic FETs, channel current flows in lateral direction (parallel to the substrate surface), in-plane π-stacking with an edge-on orientation is desired. Treating the gate insulator by SAM such as octadecyltrichlorosilane (OTS-18), octyltrichlorosilane (OTS-8), or hexamethyldisilizane (HMDS) is an effective approach to enhance the edge-on orientation in P3HT or poly(3, 3$'''$-didodecylquaterthiophene) (PQT-12). The alkyl chains of SAMs help to align P3HT or PQT-12 chains.[6,7] On the vertical side, there are also some reports on the effect of SAM treatment of vertical nano-pore sidewalls on the polymer morphology and mobility.[5,8–10] Such vertical sidewall treatment, however, has not been used for high-performance vertical transistor. In this work, SAM is used to modify the vertical nano-channel sidewalls in vertical transistor.[11,12] The vertical transistor output current is greatly enhanced. The SAM-treated vertical P3HT transistor, named as SAM-SCLT, delivers an output current of 50-110 mA/cm^2 (dependent on P3HT thickness) at 2 V with an on/off current ratio larger than 10 000.

The process flow to fabricate the SAM-SCLT is shown in Fig. 1(b). First, a 200-nm-thick cross-linkable poly(4-vinyl phenol) (PVP) layer is spin-coated on an indium-tin-oxide (ITO) glass substrate. Then, after modifying the PVP surface energy by coating a thin P3HT layer, the polystyrene (PS) spheres of 100 nm diameter were adsorbed on the substrate. After evaporating a 40-nm-thick aluminum (Al) layer and removing the PS spheres by a Scotch tape, a grid-like Al metal sheet with nanopores is formed. Deep nanopores are fabricated by oxygen plasma etching down the whole PVP layer through the grid-like Al as the hard mask. After treating the template with various kinds of SAMs (HMDS, OTS-8, or OTS-18, with 2-h soaking in toluene), P3HT with molecular weight of 87 000 g/mol is coated onto the template. In this study, except conventional spin-coating, we also use blade-coating without spinning to deposit P3HT. Organic light-emitting diodes fabricated by blade-coating were

a)Authors to whom correspondence should be addressed. Electronic addresses: hsiaowen@mail.nctu.edu.tw and meng@mail.nctu.edu.tw.
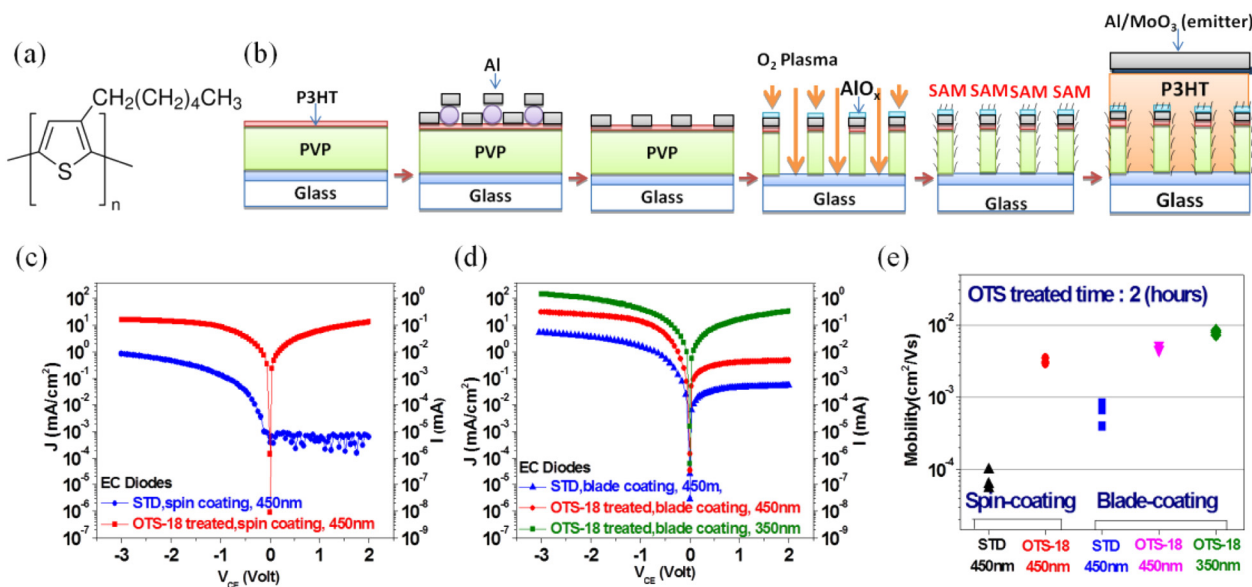
FIG. 1. (a) The chemical structure of RR-P3HT. (b) The process flow chart of fabricating vertical polymer transistors. (c) The J_C - V_{CE} characteristics of spin-coated P3HT EC diodes without and with OTS-18 treatment. (d) The J_C - V_{CE} characteristics of blade-coated P3HT EC diodes without and with OTS-18 treatment, with different P3HT thickness of 350 nm and 450 nm. (e) The hole mobility fitted from the current-voltage relation of space-charge-limited current.

reported in our previous works.[13,14] The channel length is defined by P3HT film thickness (i.e., thickness inside the nanopores plus thickness above the nanopores) as 350 nm or 450 nm. Finally, to finish the vertical transistor, a top metal containing thin molybdenum oxide (MoO_3) and Al is evaporated to serve as the emitter electrode to inject holes into P3HT. Standard glass sealing with UV-sealing glue is used to achieve encapsulation. The active area, including the nanopore structure, is 1 mm^2 and is defined by the intersection between collector electrode and emitter electrode. Characteristics of SCLT with glass sealing suffer only 0.3% degradation after 7 h in ambient and 2% degradation after 5 days in glove box (not shown). More process details are given in supporting information. The vertical transistor operates like a solid-state vacuum tube.[11,15] Holes are injected from top metal (emitter) to bottom metal (collector), while the aluminum grid metal acts as the base electrode to control the channel potential profile and to turn on or turn off the transistor.

We first compare the planar P3HT deposited by blade-coating and spin-coating. The current-voltage relationships of planar ITO/P3HT/MoO_3/Al diodes with blade-coated and spin-coated P3HT are investigated (not shown). No significant difference can be observed between these two diodes. The space-charge-limited mobilities (μ_{SCLC}), extracted by fitting the current-voltage relation with space-charge-limited current, for blade-coated P3HT and spin-coated P3HT are both around 5×10^{-4} cm^2/Vs.[6,16] The value is similar to previously reported μ_{SCLC} in P3HT diodes.[16] Then, the collector current densities as a function of collector to emitter voltage (J_C - V_{CE} plot) of the emitter-collector diodes (EC diodes) in SCLTs with P3HT nanorod structure are investigated. The current density and mobility are calculated by considering the total active area as 1 mm^2, including the nanopore structure. The nanopore structure occupies roughly 20% of the active area. If we further consider that the current only flows through nanopores, the amount of current density and mobility in this paper will be 5-times larger than the amount given

in this paper. The J_C - V_{CE} plots of spin-coated P3HT EC diodes (450-nm P3HT) without and with OTS-18 treatment are compared in Fig. 1(c). Without SAM treatment, J_C is lower than 1 mA/cm^2 at $V_{CE} = -3$ V (with holes injected from MoO_3/Al). J_C is only 10^{-3} mA/cm^2 when V_{CE} is positive (with holes injected from ITO). This may be due to the poor contact between the P3HT and ITO when P3HT fills into the nanopores. After using OTS-18 to treat the nanopore template, spin-coated P3HT diode delivers a J_C of 16.4 mA/cm^2 at $V_{CE} = -3$ V. The J_C - V_{CE} plots of blade-coated P3HT EC diodes without and with OTS-18 treatment are compared in Fig. 1(d). The output currents of blade-coated P3HT EC diodes are larger than those of spin-coated P3HT EC diodes. The hole mobility fitted from the current-voltage relation of space-charge-limited current is given in Fig. 1(e).[16,17] The effective hole mobility is 8×10^{-3} cm^2/Vs with SAM and 8×10^{-4} cm^2/Vs without SAM using blade-coating.[17] It reduces to be 9×10^{-5} cm^2/Vs using spin-coating without SAM.

Two reasons are proposed to explain the enhanced output current with OTS-18 treatment: (1) the improved nanopore-filling and (2) the improved P3HT chain ordering.

The pore-filling phenomena are first discussed. The cross sectional scanning electron microscope (SEM) images of the spin-coated and blade-coated P3HT EC diodes without OTS-18 treatment are shown in Figs. 2(a) and 2(b), respectively. While P3HT can be seen to fill into nanopores, some narrow spacings can be observed at sidewall areas. The cross sectional views of the spin-coated and blade-coated P3HT EC diodes with OTS-18 treatment are shown in Figs. 2(c) and 2(d), respectively. P3HT nanorods with clear edges are observed. The edges of the rods fit with the shape of the nanopores very well, indicating an almost completely pore-filling and thus giving rise to a good contact between ITO and P3HT.

To analyze the molecular packing in P3HT film, grading-incident x-ray diffraction (GIXRD) and photoluminescence (PL) spectroscopy are used to get more structural information
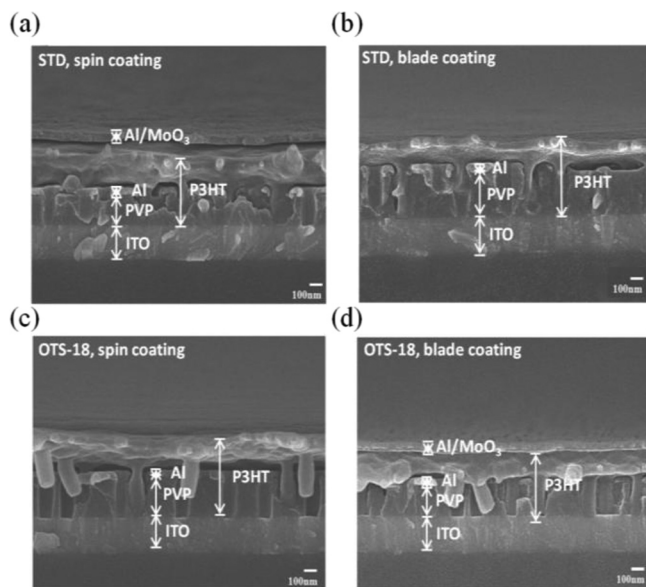
FIG. 2. SEM cross-section images of (a) the spin-coated P3HT EC diode without OTS-18 treatment; (b) the blade-coated P3HT EC diode without OTS-18 treatment; (c) the blade-coated P3HT EC diode with OTS-18 treatment; (d) the blade-coated P3HT EC diode with OTS-18 treatment.

inside the P3HT film. The out-of-pane GIXRD spectra of blade-coated P3HT on STD (without SAM) template and on OTS-18-treated template are compared in Fig. 3(a). Samples used in this analysis composed of P3HT inside nanopores and P3HT above nanopore structure as shown in the inset of Fig. 3(a). Stronger reflection of the (100) layer can be observed at $2\theta = 5.4°$ for P3HT on OTS-18-treated template, indicating enhanced π-stacking lamellar structure and edge-on orientation. The face-on orientation, represented by the reflection of the (010) layer, is not significantly influenced by OTS treatment. Since OTS-18 also bonded on the top of the porous template, the reflection signal from P3HT above the porous template may dominate the spectra in Fig. 3(a). To remove the reflection signal from P3HT above the porous template, we use oxygen plasma to etch away P3HT above the template. Only P3HT inside nanopores remained. After plasma etching, the GIXRD spectra of blade-coated P3HT on STD and on OTS-18-treated templates are compared in Fig. 3(b). The reflections of the (100) layers almost diminished, while signals from (010) layers are almost identical for both devices. It is suggested that, inside nanopores, almost no edge-on orientation is observed. The face-on orientation is observed but is not dependent on OTS treatment. The vertical orientation is not detectable in out-of-plane GIXRD. Grazing-incidence wide-angle x-ray scattering (GI-WAXS) or two-dimensional grazing-incidence x-ray diffraction (2D GIXRD) might help to analyze the vertical orientation in the rod-shaped P3HT.[5,18] We also use PL spectroscopy to analyze the molecular packing of the rod-shaped P3HT. An improved chain packing for P3HT inside OTS-treated nanopores is observed. The PL spectra of blade-coated P3HT on STD and on OTS-treated templates after plasma etching are compared in Fig. 3(c). The 0-0 to 0-1 peak intensity ratio, S_R, is usually used as a probe for disorder.[19,20] The 0-0 peak is forbidden by symmetry in aggregates. When disorder occurs, the symmetry is broken to generate 0-0 emission. In Fig. 3(c), S_R becomes lower for P3HT molecules in OTS-treated nanopores, indicating an improved molecular
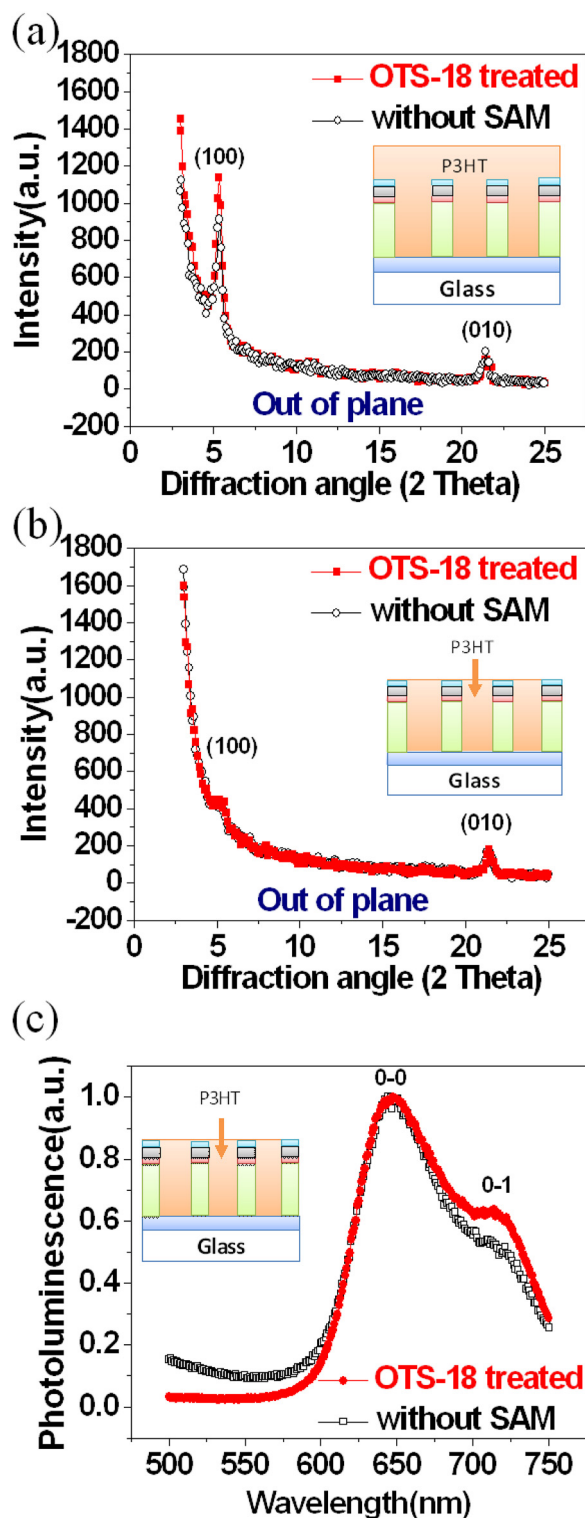

FIG. 3. (a) Out-of-plane GIXRD measurement graphs for blade-coated P3HT on STD and on OTS-18-treated templates before removing P3HT above the porous templates; (b) the graphs for the samples after using oxygen plasma to etch away P3HT above the porous template; and (c) the PL spectra of blade-coated P3HT on STD and on OTS-treated templates after plasma etching.

ordering. Since SAM does not change the intensity of face-on orientation in Fig. 3(b), we propose that the enhanced current is due to enhanced pore-filling shown in Figs. 2(a)–2(d) and the higher inter-chain order revealed in Fig. 3(c).

Finally, we compare the SCLT characteristics when SCLTs are fabricated on STD (no SAM treatment) template

and SAM-treated templates with three different SAMs. Output current densities (J_C) measured at $V_{CE} = -2.0$ V and $V_{BE} = -0.9$ V of various SCLTs are plotted in Fig. 4(a). Without SAM treatment, J_C for both spin-coated and blade-coated SCLT are below 10 mA/cm^2. Using OTS-18 treatment on template for 2 h, J_C for spin-coated SCLT and blade-coated SCLT are 20 mA/cm^2 and 50 mA/cm^2, respectively. Reducing the alkyl chain of the SAM from 18 C to 8 C (OTS-8), J_C for blade-coated SCLT is slightly reduced to be around 25 mA/cm^2. HMDS treatment does not improve J_c. Increasing the soaking time in toluene from 2 h to 4 h can slightly increase J_c of HMDS-treated SCLT, however, the insulating property of PVP is seriously degraded (not shown). It is concluded that the highest output current can be obtained for SCLTs with OTS-18-treated template and blade-coated P3HT. A J_C around 160 mA/cm^2 and on/off ratio of 5300 can be obtained when we further reduces P3HT thickness from 450 nm to 350 nm. The J_C - V_{CE} curves and the J_C - V_{BE} curves of blade-coated SCLT with OTS-18 treatment and 450-nm P3HT are shown in Figs. 4(b) and 4(c),

respectively. The total output current is also shown in the right axis. The on/off current ratio is around 10 000. Under various bias conditions, base leakage current density (J_B) is lower than 2×10^{-3} mA/cm^2 as shown in Fig. 4(c). The output current densities, the on/off current ratio and the operation voltage of SCLTs fabricated with various conditions are listed in Table SI in supporting information.

In summary, we show the importance of using self-assemble monolayer on the sidewall of vertical nanometer pores to increase the vertical conductivity of P3HT inside the nanometer pores. After treating the porous template with OTS-18, the sidewall of nanometer pores becomes hydrophobic to facilitate the pore filling of P3HT. The SAM does not change the overall polymer chain orientation but enhances the pore filling and inter-chain order. Using blade-coating instead of spin-coating to deposit P3HT on porous template further improves the vertical mobility. Finally, the SAM-treated vertical P3HT transistor delivers an output current of 50-110 mA/cm^2 (dependent on P3HT thickness) at 2 V with an on/off current ratio larger than 10 000. The output current is far more enough to drive an OLED in display application. Considering the high output current, low operation voltage and high on/off ratio, SAM-SCLT is one of the best solution-processed organic transistors.
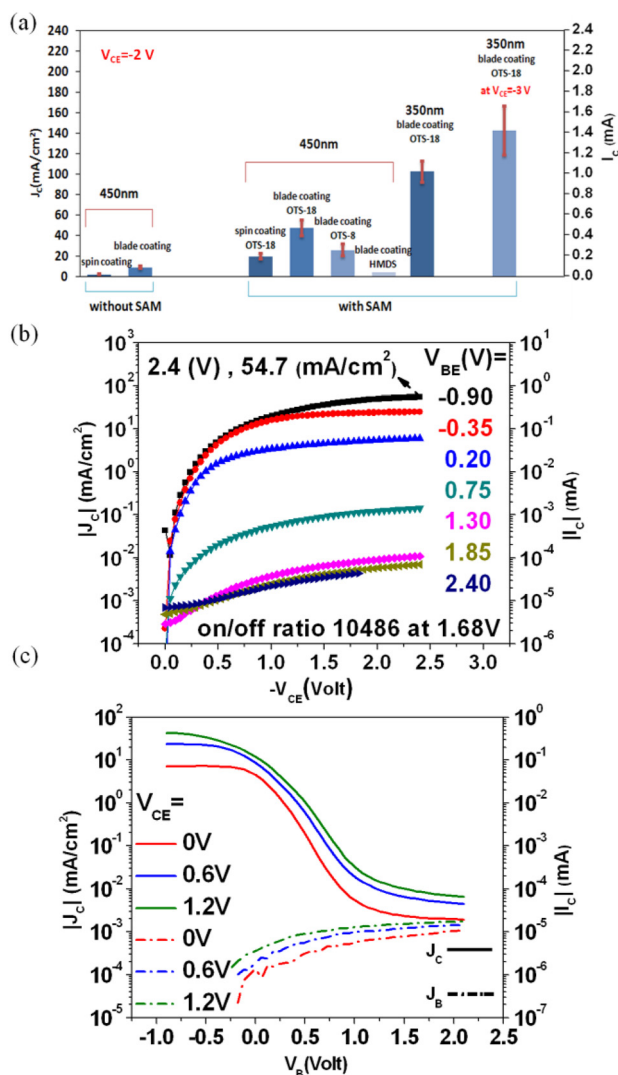
FIG. 4. (a) The average output current densities (J_C) measured at $V_{CE} = -2$ V and $V_{BE} = -0.9$ V of various SCLTs. Error bars represent the standard deviations obtained from at least 3 samples. (b) The J_C - V_{CE} curves of blade-coated SCLT with OTS-18 treatment measured at different V_{BE}. (c) The J_C - V_{BE} curves and base leakage current, J_B of blade-coated SCLT measured at different V_{CE}.

[1]Y. C. Chao, H. F. Meng, S. F. Horng, and C. S. Hsu, Org. Electron **9**, 310 (2008).
[2]Y. C. Chao, Y. C. Lin, M. Z. Dai, H. W. Zan, and H. F. Meng, Appl. Phys. Lett. **95**, 203305 (2009).
[3]H. Sirringhaus, P. J. Brown, R. H. Friend, M. M. Nielsen, K. Bechgaard, B. M. W. Langeveld-Voss, A. J. H. Spiering, R. A. J. Janssen, E. W. Meijer, P. Herwig, and D. M. de Leeuw, Nature **401**, 685 (1999).
[4]H. Sirringhaus, R. J. Wilson, R. H. Friend, M. Inbasekaran, W. Wu, E. P. Woo, M. Grell, and D. D. C. Bradley, Appl. Phys. Lett. **77**, 406 (2000).
[5]M. Aryal, K. Trivedi, and W. C. Hu, ACS Nano **3**, 3085 (2009).
[6]C. Goh, R. J. Kline, M. D. McGehee, E. N. Kadnikova, and J. M. J. Fréchet, Appl. Phys. Lett. **86**, 122110 (2005).
[7]R. J. Kline, M. D. Mcgehee, and M. F. Toney, Nature Mater. **5**, 222 (2006).
[8]D. Mcbranch, I. H. Campbell, D. L. Smith, and J. P. Ferraris, Appl. Phys. Lett. **66**, 1175 (1995).
[9]K. M. Coakley, B. S. Srinivasan, J. M. Ziebarth, C. Goh, Y. X. Liu, and M. D. McGehee, Adv. Funct. Mater. **15**, 1927 (2005).
[10]J. S. Kim, Y. Park, D. Y. Lee, J. H. Lee, J. H. Park, J. K. Kim, and K. Cho, Adv. Funct. Mater. **20**, 540 (2010).
[11]Y. C. Chao, H. F. Meng, and S. F. Horng, Appl. Phys. Lett. **88**, 223510 (2006).
[12]Y. C. Chao, C. H. Chung, H. W. Zan, H. F. Meng, and M. C. Ku, Appl. Phys. Lett. **99**, 233308 (2011).
[13]S. R. Tseng, H. F. Meng, K. C. Lee, and S. F. Horng, Appl. Phys. Lett. **93**, 153308 (2008).
[14]C. Y. Chen, H. W. Chang, Y. F. Chang, B. J. Chang, Y. S. Lin, P. S. Jian, H. C. Yeh, H. T. Chien, E. C. Chen, Y. C. Chao, H. F. Meng, H. W. Zan, H. W. Lin, S. F. Horng, Y. J. Cheng, F. W. Yen, I. F. Lin, H. Y. Yang, K. J. Huang, and M. R. Tseng, J. Appl. Phys. **110**, 094501 (2011).
[15]Y. C. Chao, M. C. Ku, W. W. Tsai, H. W. Zan, H. F. Meng, H. K. Tsai, and S. F. Horng, Appl. Phys. Lett. **97**, 223307 (2010).
[16]M. Giulianini, E. R. Waclawik, J. M. Bell, and N. Motta, J. Appl. Phys. **108**, 014512 (2010).
[17]See supplementary material at http://dx.doi.org/10.1063/1.4748284 for details about mobility extraction.
[18]J. E. Allen, K. G. Yager, H. Hlaing, C. Y. Nam, B. M. Ocko, and C. T. Black, Appl. Phys. Lett. **99**, 163301 (2011).
[19]J. Clark, C. Silva, R. H. Friend, and F. C. Spano, Phys. Rev. Lett. **98**, 206406 (2007).
[20]F. C. Spano, J. Clark, C. Silva, and R. H. Friend, J. Chem. Phys. **130**, 074904 (2009).